

Self-assembly of manganese phthalocyanine on Pb(111) surface: A scanning tunneling microscopy study

Dan Hao,¹ Canli Song,¹ Yanxiao Ning,² Yilin Wang,² Lili Wang,² Xu-Cun Ma,² Xi Chen,¹ and Qi-Kun Xue^{1,a)}

¹Department of Physics, Tsinghua University, Beijing 100084, China

²Institute of Physics, Chinese Academy of Sciences, Beijing 100190, China

(Received 2 January 2011; accepted 29 March 2011; published online 15 April 2011)

The self-assembled structure of submonolayer manganese phthalocyanine (MnPc) on Pb(111) surface is investigated by using low-temperature scanning tunneling microscopy (STM). A “holelike” superlattice, which is superimposed on the self-assembled nearly quadratic network, is observed. High resolution STM images reveal that there are two distinct azimuthal orientations of MnPc molecules. It is found that by taking the two different orientations the self-assembly can further be optimized energetically by maximizing intermolecular orbital overlapping. It is this intralayer energy minimization process that leads to the characteristic holelike superlattice. © 2011 American Institute of Physics. [doi:10.1063/1.3579493]

Understanding the self-assembled structure of organic molecules on single crystalline metal substrate is of great importance due to technological and fundamental interests of molecular thin films.^{1–3} Metal phthalocyanine (MPc), whose structure is shown schematically in Fig. 1(a), and their derivatives show many fascinating applications, such as organic semiconductor optoelectronic devices, catalysis, and solar cells,^{4–8} their self-assembly has extensively been studied. Due to high spatial resolution capability, scanning tunneling microscope (STM) has proven a powerful technique for investigating the geometric conformations of MPc on various metal substrates in the past few decades.^{9–17} Two distinctive STM image contrasts dependent of the central metal atom, such as Cu, Ni, Co, and Fe, were revealed, which represent the specific metallic *d*-orbital occupations in the corresponding MPc molecules.^{10,18} Recent inspection of the MPc geometry indicates that MPc molecules tend to form a quadratic or nearly quadratic lattice due to stronger molecule–molecule interaction and the intrinsic fourfold symmetry of the molecules. Hexagonal lattices are obtained in some experimental conditions,^{16–19} which results from much stronger molecule–substrate interaction. In this case, the geometry of the self-assembled structure is largely determined by that of the metal substrate.

The different overlayer structures have often been explained in terms of a subtle balance between the intralayer energy determined by the molecule–molecule interaction and the overlayer–substrate interface energy. According to the classification of Hooks *et al.*,² a commensurate epitaxial relationship between the overlayer and substrate will form when stronger molecule–substrate interaction is involved and the elastic constant of the overlayer is smaller than that of the overlayer–substrate interface. The elastic constant is proportional to the second derivative at the minima of the corre-

sponding potential energy function. In contrary, an incommensurate overlayer will appear if the elastic constant of the overlayer is greatly bigger than that of the overlayer–substrate interface. If the elastic constant of the overlayer is comparable to that of the overlayer–substrate interface, more complicated structures such as point-on-line coincidence, geometrical coincidence, and line-on-line coincidence form.^{13,20} Therefore, an STM study of the self-assembled molecular structures provides an effective approach to understanding the intermolecular interaction and molecule–substrate interaction as well as their competition at atomic level.

In the present study, we have investigated the self-assembled structure of submonolayer MnPc molecules on Pb(111) by using STM. The STM observation reveals a characteristic superstructure made of dark holes that are superimposed on the assembled quadratic structure. By studying bias-dependent high resolution STM images and by comparison to cobalt phthalocyanine (CoPc) molecules, we find that the formation mechanism is different from those reported in previous studies.^{14,21} We show that the long-ranged ordered holes can be understood in terms of intralayer energy minimization via two distinct azimuthal orientations, and relative arrangements of the molecules.

Our experiments were conducted in a commercial Unisoku ultrahigh vacuum low-temperature STM system with a base pressure of 2×10^{-10} Torr. A molecular beam epitaxy (MBE) chamber connected to the STM chamber was used for *in situ* preparation of samples. The Pb(111) substrate was obtained by depositing nominal three to four monolayers (ML) 99.999% Pb on the Si(111)- $\sqrt{3} \times \sqrt{3}$ R30°-Pb surface.²² The MnPc molecules (Aldrich Inc.) were thermally sublimated from a homemade Ta boat heated to 600 K onto the Pb substrate. During the deposition, the substrate was kept at room temperature (RT). The condition results in a low deposition rate of approximately 0.01 ML per min, and the resulted self-assembled molecular monolayer is more or less a thermodynamically stable structure. STM topographic images

^{a)} Author to whom correspondence should be addressed. Electronic mail: qkxue@mail.tsinghua.edu.cn.

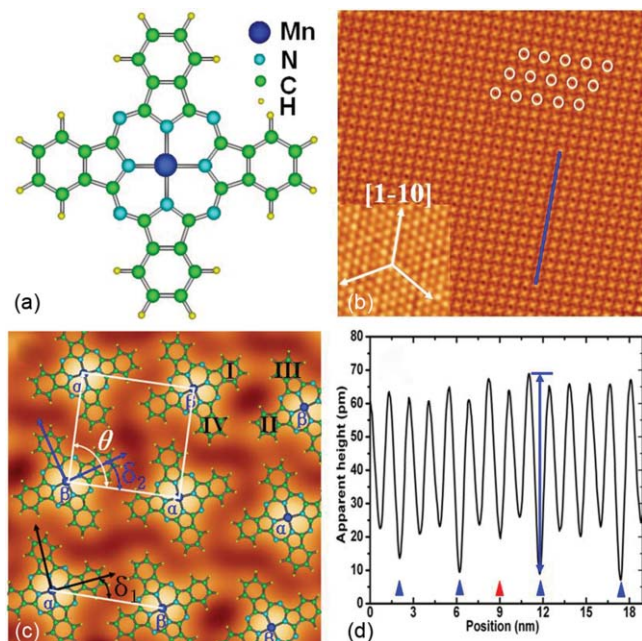


FIG. 1. (a) Schematic structure model of MnPc molecule. (b) Large-scale STM image obtained after depositing 0.8 ML MnPc molecules on Pb(111) at RT. The white circles highlight the location of the dark holes, which forms a hexagonal lattice. The inset (4×4 nm) shows the atomic resolution image of the underlying Pb(111) surface. The three white arrows represent the close-packed directions of the Pb(111) substrate. (c) High-resolution STM image superimposed with the molecule model. The black and blue arrows indicate the molecular axes in α and β orientations, respectively. (d) A cross-sectional profile along the blue line in Fig. 1(b). Image bias and size: (b) 0.2 V, 40×40 nm and (c) 0.1 V, 4×4 nm.

were taken at 80 K with a constant current of 0.1 nA. The features recorded with positive bias voltage reflect the unoccupied electronic states of the sample. The measurements were calibrated based on both Si (111)- 7×7 reconstruction surface and the atom resolved image of the Pb(111) surface at 80 K. Polycrystalline PtIr or tungsten tips after e-beam heating in the MBE chamber were used for STM measurements. The STM images were processed using the WSXM software.²³

Figure 1(b) shows a typical STM image after deposition of 0.8 ML MnPc on the Pb(111) surface. The sample bias voltage is 0.2 V. The atomically resolved STM image of the uncovered Pb(111) surface is shown in the inset of Fig. 1(b), from which the close-packed directions (white arrows) of the underlying Pb substrate can clearly be seen. From Fig. 1(b), the quadratic arrangement of MnPc is immediately evident. The nearly quadratic unit cell is outlined by a white square in Fig. 1(c). Interestingly, there also exists a well-ordered superstructure of dark holes (the white circles), which extends several hundred nanometers. We note that the close-packed directions (blue line) of the assembled molecules deviates slightly by $\sim 2^\circ$ from the close-packed direction of the Pb substrate. As shown by the zoom-in STM image in Fig. 1(c), each molecule is imaged as a four-lobe feature, suggesting a flat-lying configuration of MnPc on Pb(111). The central bright protrusion results from the highly occupied $3d$ orbitals of the Mn atom. The observation is consistent with the structure model in Fig. 1(a) and the previous reports of MnPc molecules on other substrates.^{11–19}

By statistical analysis of several tens STM images and the corresponding fast Fourier transformation (FFT), the lattice parameters of the MnPc overlayer are determined to be $a = 1.40$ nm, $b = 1.39$ nm, and $\theta = 94 \pm 3^\circ$. From the parameters, we can deduce the following epitaxial relationship between the MnPc overlayer and the Pb(111) substrate,

$$\begin{pmatrix} a \\ b \end{pmatrix} = \begin{pmatrix} 3.96 & -0.08 \\ -1.94 & 4.57 \end{pmatrix} \begin{pmatrix} a_0 \\ b_0 \end{pmatrix},$$

where (a, b) and (a_0, b_0) indicate the unit cell vectors of the MnPc overlayer and the Pb(111) surface, respectively. In terms of the measurement errors, the two quasi-integers in the first column of the matrix do not necessarily suggest that the molecules form the well-known point-on-line coincidence with the underlying Pb lattice.² This problem will be discussed later on.

The dark holes in Fig. 1(b) form a hexagonal lattice with its close-packed directions rotated by 30° with respect to those of the substrate lattice. This observation is independent of the bias voltage from -4.0 to 2.0 V, suggesting that the dark holes are unlikely from electronic effect. Tip artifacts are excluded by using different tips and samples. According to the cross-sectional profile [refer to the blue line in Fig. 1(b)] in Fig. 1(d), the holes appear darker by an apparent contrast of ~ 15 pm compared to the depression between two neighboring molecules. In Fig. 1(d), the location of the holes is indicated by blue arrows while that of the usual depression by a red arrow.

By superimposing the molecular model on the high resolution STM image [Fig. 1(c)], we find that the molecules take two distinct in-plane azimuthal orientations, denoted as α and β orientations, respectively. The angles δ_1 and δ_2 between one of the molecular axes and the lattice vector in α and β orientations are determined to be $25 \pm 3^\circ$ and $35 \pm 3^\circ$, respectively. The angles are comparable with the value for other MPC molecules on metal substrates (between 14° and 36.5°).^{16,19,24} A surprising result is that the holes exclusively occur between two neighboring molecules with β -orientation, which is different from the regularly ordered faults in previous studies.^{14,20} Therefore, we can correlate the ordered holes with different stacking of the molecules at different orientations. Among three stacking configurations (namely, α - α , α - β , and β - β) along the close-packed direction, a largest distance between the benzene rings [for example, ring I and ring II marked in Fig. 1(c)] of the neighboring molecules is found in the β - β configuration. It should be pointed out that the areal density of the molecules is equal for three stacking configurations, suggesting that the molecule-substrate interaction and the resulted energy gain is the same for three configurations. Since the larger distance means lesser orbital overlapping between the benzenes and thus weaker molecule-molecule interactions, the observation seems to suggest that the β - β configuration may represent a less stable structure compared to α - α and α - β .

However, careful inspection of the high resolution STM images reveals different features. Figure 2(a) shows a filled state STM image recorded at a negative bias of -0.5 V. The image shows more features in the regions between the molecules, where the intermolecular orbital overlapping

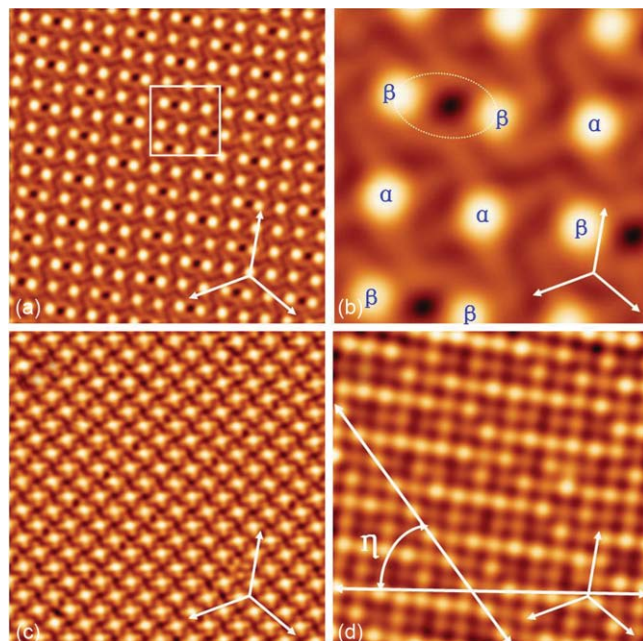


FIG. 2. (a) A typical STM image of the self-assembled MnPc monolayer taken at a negative bias of -0.5 V. (b) The zoom-in STM image of (a) the dotted white ellipse shows the orbital overlapping of molecules in the β - β configuration. (c) STM image of CoPc monolayer on Pb(111) taken at a bias of -0.5 V. (d) Optimal image of Fig. 2(a) via wavelet analysis. Image size: (a), (c), and (d) 20×20 nm, (b) 4×4 nm.

should occur. Notably, around the hole there exists stronger orbital overlapping between two molecules in the β - β configuration. The contrast between the two pairs of benzene rings of the molecules forming β - β configuration is brighter than those of the α - α and α - β configurations, implying stronger bonding is formed in the β - β configuration. This situation is illustrated by the dotted ellipse in Fig. 2(b). On the other hand, in α - α and α - β configurations, the four-lobe feature remains as an isolated molecule. It is now clear that by increasing the distance between benzene ring I and ring II with molecule in-plane rotation, the orbital overlapping between ring I and ring III and between ring II and ring IV is enhanced. It should lead to a larger energy gain for the β - β configuration. In the case of CoPc on Pb(111) where all molecules take the same orientation, the four-lobe feature of each molecule is clearly seen under the same imaging conditions [Fig. 1(c)].

To further understand the overlayer structure, we performed wavelet analysis transform of Fig. 2(a).²⁵ The result is shown in Fig. 2(d), where a well-defined Moiré-like pattern is observed. The supercell orientations of the Moiré pattern are depicted by two white arrows with an angle of $\eta = 54 \pm 3^\circ$. Note that the Moiré-like pattern can be acquired for any STM images taken with different sample bias after the similar optimization. The modulated contrasts are expected to be correlated to the different registry sites of the molecules with respect to the underlying substrate atoms. The Moiré pattern suggests that MnPc molecules form an incommensurate structure. It indicates a rather weak molecule-substrate interaction and that the dominant driving force for molecular assembling is the intermolecular interaction.

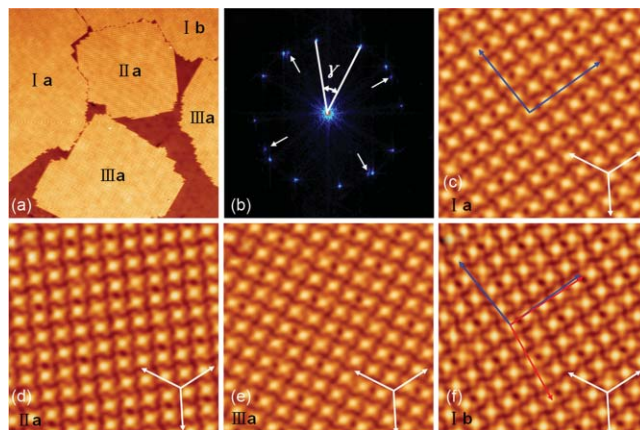


FIG. 3. (a) STM image showing different domains of self-assembled MnPc monolayer. (b) The FFT image of Fig. 3(a). (c-f) STM images showing the structures of Ia, IIa, IIIa, and Ib domains. The blue and red arrows indicate the molecular packing directions in Ia and Ib domains, respectively. All images were obtained with a sample bias of 0.34 V except 1.0 V for Fig. 3(a). Image size: (a) 150×150 nm, (c-f) 15×15 nm.

Figure 3(a) shows a large-scale STM image where five domains are present. The representative zoom-in images taken in the domains of Ia, IIa, IIIa, and Ib are depicted in Figs. 3(c)-3(f), respectively. Labels I, II, and III represent three symmetry-equivalent structures, while the subscripts a and b denote the variants induced by the noncoincidence between the molecular packing axes and the close-packed directions of Pb substrate. The close-packed directions of the holes in all domains form an angle of $120 \pm 3^\circ$ with respect to each other, as clearly seen in the STM images from Fig. 3(c) to Fig. 3(e). In terms of the threefold symmetry of the Pb substrate, the observation suggests that the molecule-substrate interaction still plays some roles although it is weak as discussed above. Fig. 3(b) is a 2D-FFT image of Fig. 3(a), from which three equivalent domain structures can be more obviously identified.^{17,26} Here, it is worthy to point out two features. One is that the first-order reciprocal spots do not form the expected regular 12-fold pattern. The measured angles between any neighboring spots [for example, γ in Fig. 3(b)] vary from 24° to 36° . The second is occurrence of darker spots with fourfold symmetry, as indicated by the arrows in Fig. 3(b). Such spots come from Ib domain, which is correlated with Ia domain via mirror symmetry. The results further suggest that the overlayer is incommensurate with the substrate, in agreement with the above wavelet analysis.

In summary, we have investigated the self-assembled structure of MnPc molecules on Pb(111) surface by using STM. A very intriguing superstructure of dark holes is observed. By careful inspection of the high resolution STM images, a new mechanism for self-assembling of metal phthalocyanine molecules is identified. By taking different azimuthal orientations, the intermolecular orbital overlapping is enhanced so that the surface energy can be further minimized.

¹J. K. Gimzewski and C. Joachim, *Science* **283**, 1683 (1999).

²D. E. Hooks, T. Fritz, and M. D. Ward, *Adv. Mater.* **13**, 227 (2001).

³M. Ermtchenko, J. A. Schaefer, and F. S. Tautz, *Nature (London)* **425**, 602 (2003).

⁴G. Witte and C. J. Wöll, *J. Mater. Res.* **19**, 1889 (2004).

- ⁵S. Baranton, C. Countanceau, C. Roux, F. Hahn, and J. M. Leger, *J. Electroanal. Chem.* **577**, 526 (2005).
- ⁶K. Arihara, L. Q. Mao, P. A. Liddell, E. Marino-Ochoa, A. L. Moore, T. Imase, D. Zhang, T. Sotomura, and T. Ohsaka, *J. Electrochem. Soc.* **7**, A2047 (2004).
- ⁷A. K. Ghosh, D. L. Morel, T. Feng, R. F. Rowe, and C. A. Rowe, *J. Appl. Phys.* **45**, 230 (1974).
- ⁸Y. Amao and T. Komori, *Langmuir* **19**, 8872 (2003).
- ⁹P. H. Lippel, R. J. Wilson, M. D. Miller, Ch. Wöll, and S. Chiang, *Phys. Rev. Lett.* **62**, 171 (1989).
- ¹⁰K. W. Hipps, X. Lu, X. D. Wang, and U. Mazur, *J. Phys. Chem.* **100**, 11207 (1996).
- ¹¹S. Berner, M. de Wild, L. Ramoino, S. Ivan, A. Baratoff, H. J. Guntherodt, H. Suzuki, D. Schlettwein, and T. A. Jung, *Phys. Rev. B* **68**, 115410 (2003).
- ¹²M. Takada and H. Tada, *Chem. Phys. Lett.* **392**, 265 (2004).
- ¹³S. C. B. Mannsfeld and T. Fritz, *Phys. Rev. B* **71**, 235405 (2005).
- ¹⁴M. Koudia, M. Abel, C. Maurel, A. Blik, D. Catalin, M. Mossoyan, J. C. Mossoyan, and L. Porte, *J. Phys. Chem. B* **110**, 10058 (2006).
- ¹⁵Y. Wakayama, *J. Phys. Chem. C* **111**, 2675 (2007).
- ¹⁶J. Ahlund, J. Schnadt, K. Nilson, E. Gothelid, J. Schiessling, F. Besenbacher, N. Martensson, and C. Puglia, *Surf. Sci.* **601**, 3661 (2007).
- ¹⁷Z. H. Cheng, L. Gao, Z. T. Deng, N. Jiang, Q. Liu, D. X. Shi, S. X. Du, H. M. Guo, and H. J. Gao, *J. Phys. Chem. C* **111**, 9240 (2007).
- ¹⁸D. E. Barlow and K. W. Hipps, *J. Phys. Chem. B* **104**, 5993 (2000).
- ¹⁹T. G. Gopakumar, M. Lackinger, M. Hackert, F. Müller, and M. Hietschold, *J. Phys. Chem. B* **108**, 7839 (2004).
- ²⁰S. C. B. Mannsfeld, K. Leo, and T. Fritz, *Phys. Rev. Lett.* **94**, 056104 (2005).
- ²¹V. Oison, M. Koudia, M. Abel, and L. Porte, *Phys. Rev. B* **75**, 1098 (2007).
- ²²Y. S. Fu, S. H. Ji, X. Chen, X. C. Ma, R. Wu, C. C. Wang, W. H. Duan, X. H. Qiu, B. Sun, P. Zhang, J. F. Jia, and Q. K. Xue, *Phys. Rev. Lett.* **99**, 256601 (2007).
- ²³I. Horcas, R. Fernandez, J. M. Gomez-Rodriguez, J. Colchero, J. Gomez-Herrero, and A. M. Baro, *Rev. Sci. Instrum.* **78**, 013705 (2007).
- ²⁴M. Lackinger, T. Müller, T. G. Gopakumar, F. Müller, M. Hietschold, and G. Flynn, *J. Phys. Chem. B* **108**, 2279 (2004).
- ²⁵C. M. Liu, L. W. Chen, and C. C. Wang, *Nonotechnology* **17**, 4359 (2006).
- ²⁶K. K. Okudaira, S. Hasegawa, H. Ishii, K. Seki, Y. Harada, and N. J. Ueno, *J. Appl. Phys.* **85**, 6453 (1999).